

# 1,3-Dipolar Cycloadditions of Diazomethane to Chiral Electron-Deficient Olefins: The Origin of the $\pi$ -Facial Diastereoselection

Elena Muray,<sup>†</sup> Angel Alvarez-Larena,<sup>‡</sup> Joan F. Piniella,<sup>‡</sup> Vicenç Branchadell,<sup>\*,†</sup> and Rosa M. Ortuno<sup>\*,†</sup>

Departament de Química, and Unitat de Cristal·lografia, Universitat Autònoma de Barcelona, 08193 Bellaterra, Barcelona, Spain

Received August 2, 1999

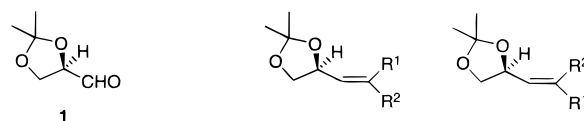
The stereochemical outcome of diazomethane cycloadditions to several chiral electron-deficient olefins has been investigated in order to establish the origin of the  $\pi$ -facial diastereoselection. Nitro olefins, vinyl sulfones, enoates, and 2-amino enoates have been used for such a purpose. These substrates have been prepared from D-glyceraldehyde acetonide through Wittig-type condensations and present an alkoxy substituent, provided by the bulky dioxolane ring, attached to the stereogenic allylic carbon. Syn-adducts have been obtained in all cases as the major isomers, independently of the *Z/E* stereochemistry of the double bond and the number and the nature of the substituents, the chirality of the asymmetric allylic carbon being the only thing responsible for the diastereoselection. Theoretical calculations show that steric hindrance due to the bulky dioxolane group is the main factor governing the preference for the syn-attack of diazomethane to the olefinic double bond.

## Introduction

Cyclopropanation of electron-deficient olefins by means of 1,3-dipolar cycloadditions of diazomethane, affording pyrazolines that under photolysis give cyclopropanes, is a method widely employed in organic synthesis. The use of chiral olefins to induce the absolute configuration of the cyclopropane stereogenic centers confers on this protocol a great versatility in the synthesis of natural or unnatural enantiopure cyclopropane derivatives.<sup>1</sup> The control of the  $\pi$ -facial diastereoselection in the cycloaddition is, therefore, crucial to obtain the target molecules with high stereoselectivity.

Several theoretical models and empiric relationships have been suggested to rationalize the origin of the diastereoselection in the cycloadditions of several dipoles to chiral olefins. Thus, for instance, the principle of 1,3-allylic strain<sup>2</sup> or the *inside alkoxy* theory<sup>3</sup> has been successfully invoked to rationalize the selectivity of many 1,3-dipolar cycloadditions. Nevertheless, these models do not apply to all kind of dipoles and dipolarophiles. Esters *Z/E-2* (Chart 1) and related  $\gamma$ -alkoxy- $\alpha,\beta$ -unsaturated esters have been extensively used in the investigation of  $\pi$ -facial diastereoselectivity in 1,3-dipolar cycloadditions. Anti isomers predominate when these compounds add to

## Chart 1



$R^1 = \text{NO}_2, R^2 = \text{Me}$	<b>Z-2</b>	<b>E-2</b>
$R^1 = \text{SO}_2\text{Ph}, R^2 = \text{H}$	<b>Z-3</b>	<b>E-3</b>
$R^1 = \text{CO}_2\text{Me}, R^2 = \text{H}$	<b>Z-4</b>	<b>E-4</b>
$R^1 = \text{CO}_2\text{Et}, R^2 = \text{Me}$	<b>Z-5</b>	<b>E-5</b>
$R^1 = \text{NHCbz}, R^2 = \text{CO}_2\text{Me}$	<b>Z-6</b>	<b>E-6</b>
$R^1 = \text{NHAc}, R^2 = \text{CO}_2\text{Me}$	<b>Z-6a</b>	<b>E-6a</b>

azomethyne ylides,<sup>4a,b</sup> nitrones,<sup>4a,c</sup> and nitrile oxides,<sup>4a,d</sup> whereas syn isomers result from the addition to nitrilimines,<sup>4e</sup> silyl nitronates,<sup>4f</sup> diazomethane,<sup>4g,h</sup> and other diazo compounds.<sup>4h</sup>

The model stated by Houk and based on the inside alkoxy effect has been applied to predict the stereochemical outcome of several concerted processes, including Diels–Alder reactions<sup>5</sup> and 1,3-dipolar cycloadditions. A good agreement between theoretical predictions and experimental results was found for the reactions between nitrile oxide and chiral allylic alcohols and ethers<sup>3a</sup> and for the cycloadditions of nitrones to  $\gamma$ -alkoxy- $\alpha,\beta$ -unsaturated esters.<sup>4c</sup> In contrast, for the addition of diazo-

\* Corresponding authors. E-mail: (V.B.) vicenc@klington.uab.es. (R.M.O.) rosa.ortuno@uab.es.

<sup>†</sup> Departament de Química.

<sup>‡</sup> Unitat de Cristal·lografia.

(1) (a) Jiménez, J. M.; Rifé, J.; Ortuno, R. M. *Tetrahedron: Asymmetry* **1996**, *7*, 537. (b) Jiménez, J. M.; Ortuno, R. M. *Tetrahedron: Asymmetry* **1996**, *7*, 3203. (c) Martín-Vilà, M.; Hanafi, N.; Jiménez, J. M.; Alvarez-Larena, A.; Piniella, J. F.; Branchadell, V.; Oliva, A.; Ortuno, R. M. *J. Org. Chem.* **1998**, *63*, 3581.

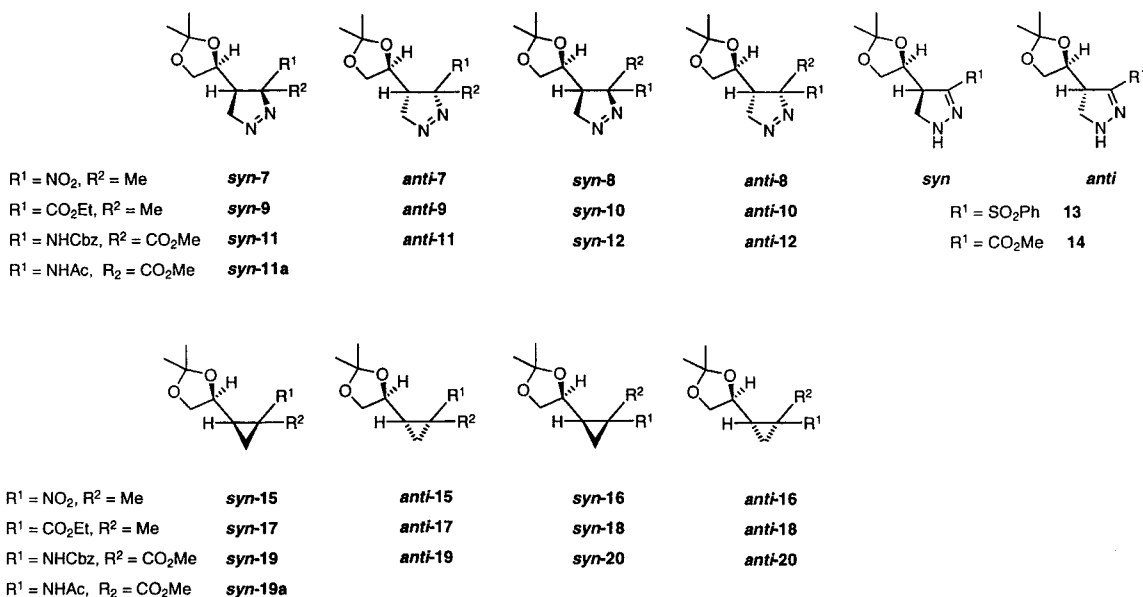
(2) (a) Hoffmann, R. W. *Chem. Rev.* **1989**, *89*, 1841. (b) Broeker, J. L.; Hoffmann, R. W.; Houk, K. N. *J. Am. Chem. Soc.* **1991**, *113*, 5006.

(3) (a) Houk, K. N.; Moses, S. R.; Wu, Y.-D.; Rondan, N. G.; Jäger, V.; Schohe, R.; Fronczek, F. R. *J. Am. Chem. Soc.* **1984**, *106*, 3880. (b) Houk, K. N.; Duh, H.-Y.; Wu, Y.-D.; Moses, S. R. *J. Am. Chem. Soc.* **1986**, *108*, 2754. (c) Raimondi, L.; Wu, Y.-D.; Brown, F. K.; Houk, K. N. *Tetrahedron Lett.* **1992**, *33*, 4409.

(4) (a) Annunziata, R.; Benaglia, M.; Cinquini, M.; Raimondi, L. *Tetrahedron* **1993**, *49*, 8629. (b) Galley, G.; Liebscher, J.; Pätz, M. *J. Org. Chem.* **1995**, *60*, 5005. (c) Busqué, F.; de March, P.; Figueredo, M.; Font, J.; Monsalvatje, M.; Virgili, A.; Alvarez-Larena, A.; Piniella, J. F. *J. Org. Chem.* **1996**, *61*, 8578. (d) Jäger, V.; Müller, I.; Schohe, R.; Frey, M.; Ehrler, R.; Häfele, B.; Schröter, D. *Lect. Heterocycl. Chem.* **1985**, *8*, 79. (e) Grubert, L.; Galley, G.; Pätz, M. *Tetrahedron: Asymmetry* **1996**, *7*, 1137. (f) Galley, G.; Jones, P. G.; Pätz, M. *Tetrahedron: Asymmetry* **1996**, *7*, 2073. (g) Annunziata, R.; Benaglia, M.; Cinquini, M.; Cozzi, F.; Raimondi, L. *Electronic Conference on Heterocyclic Chemistry (ECHET96)*. CD-ROM included in *J. Chem. Soc., Chem. Commun.* **1997**, no 6. (h) Galley, G.; Pätz, M.; Jones, P. G. *Tetrahedron* **1995**, *51*, 1631.

(5) Haller, J.; Niwayama, S.; Duh, H.-Y.; Houk, K. N. *J. Org. Chem.* **1997**, *62*, 5728.

Chart 2



methane to similar dipolarophiles, the sense of diastereoselectivity is opposite to that predicted by Houk's model.<sup>1c,4g,h</sup> A similar result was found in the cycloadditions of nitrones to chiral allyl ethers, the stereoselectivity being rationalized in these cases by means of the so-called *outside alkoxy* model suggested by Raimondi.<sup>6</sup>

On the other hand, the predominant stereochemistry observed in the cycloaddition of diazomethane to chiral  $\gamma$ -amino- $\alpha,\beta$ -dehydro amino acid esters is not explained by the 1,3-allylic strain, being necessary to consider the transition states to rationalize the factors controlling the diastereoselectivity.<sup>7</sup>

In this paper we present the results of our studies on the 1,3-dipolar cycloaddition of diazomethane to several *Z/E* chiral olefins conjugated to a nitro, sulfone, ester, or  $\alpha$ -amino ester group, the double bond being di- or trisubstituted and owning in all cases an alkoxy substituent at the allylic position. All these olefins have been synthesized from *D*-glyceraldehyde as a source of chirality. In this work, we rationalize the influence on the diastereoselection of factors such as the chirality of the stereogenic center in the substrates, the *Z/E* geometry of the double bond, the nature of the conjugated substituents, and the mono or di-substitution at the olefinic C1. The experimental results have been rationalized by theoretical calculations, allowing us to state the origin of stereoselectivity involved in this kind of cycloadditions.

## Results and Discussion

### 1. Cycloaddition Reactions and Stereochemical Assignments.

Olefins **2–6**, as pure *Z* or *E* diastereomers, were prepared according to methods described in the bibliography. In all cases, *D*-glyceraldehyde **1** was the chiral precursor bearing the chiral center (*S* configuration) which must induce  $\pi$ -facial diastereoselection in the addition of diazomethane. The methods used involve nitroaldol reaction between **1** and nitroethane to give

**Table 1. Syn/Anti Diastereomeric Excess (% de) in the Addition of Diazomethane to Olefins 2–7**

Z-olefin	pyrazolines	% de <sup>a</sup>	E-olefin	pyrazolines	% de <sup>a</sup>
<b>2</b>	<b>7</b>	84	<b>2</b>	<b>8</b>	82
<b>3</b>	<b>13</b>	>95	<b>3</b>	<b>13</b>	>95
<b>4</b>	<b>14</b>	96	<b>4</b>	<b>14</b>	96
<b>5</b>	<b>9</b>	86	<b>5</b>	<b>10</b>	84
<b>6</b>	<b>11</b>	100	<b>6</b>	<b>12</b>	100

<sup>a</sup> Determined by 250-MHz <sup>1</sup>H NMR.

olefins *Z*- and *E*-**2**,<sup>8</sup> and Wittig or Wittig–Horner condensations for the preparation of sulfones *Z*-**9** and *E*-**3**,<sup>10</sup> esters *Z*- and *E*-**4**,<sup>11</sup> *Z*-**12** and *E*-**5**,<sup>13</sup> and amino esters *Z*- and *E*-**6**<sup>1a</sup> (Chart 1).

Cycloadditions of diazomethane to these substrates were achieved in nearly quantitative yield, affording  $\Delta^1$ -pyrazolines **7–12** from 1,1-disubstituted olefins **2**, **5**, and **6**, and  $\Delta^2$ -pyrazolines **13** and **14** from 1-substituted olefins **3** and **4**, respectively (Chart 2. See therein the structures for syn/anti isomers). It is noteworthy that syn adducts were the major products in all cases independent of *Z/E* geometry, anti-adducts not being detected for amino esters **6**.<sup>1a</sup> Diastereomeric excesses were determined by NMR and are shown in Table 1. Sulfone **3**, in both *Z* and *E* isomeric forms, afforded the same *syn*- $\Delta^2$ -pyrazoline **13**. Similarly, *Z*- and *E*-esters **4** gave **14**.<sup>1c</sup>

In earlier works, we assigned unambiguously syn configuration to the major pyrazoline **14** obtained from esters **4**<sup>1c</sup> and to the only pyrazoline *syn*-**11** obtained from amino ester *Z*-**6**,<sup>1a</sup> by means of X-ray analysis.<sup>14</sup> Compound **11** was an oily material which was derivatized to solid thiocarbonate **27** according to the procedure shown

(8) Galley, G.; Hübner, J.; Anklam, S.; Jones, P. G.; Pätzl, M. *Tetrahedron Lett.* **1996**, *37*, 6307.

(9) Shahak, I.; Almog, J. *Synthesis* **1970**, 145.

(10) Craig, D.; Ley, S. V.; Simpkins, N. S. *J. Chem. Soc., Perkin Trans. 1* **1985**, 1949.

(11) Mann, J.; Partlett, N. K.; Thomas, A. *J. Chem. Res. (S)* **1987**, 369.

(12) Trost, B. M.; Reiffen, M.; Crimmin, M. *J. Am. Chem. Soc.* **1979**, *101*, 259.

(13) Ibuka, T.; Akimoto, N.; Tanaka, M.; Nishii, S.; Yamamoto, Y. *J. Org. Chem.* **1989**, *54*, 4055.

(14) Jiménez, J. M.; Casas, R.; Ortuño, R. M. *Tetrahedron Lett.* **1994**, *32*, 5945.

(6) Annunziata, R.; Benaglia, M.; Cinquini, M.; Cozzi, F.; Raimondi, L. *Eur. J. Org. Chem.* **1998**, 1823.

(7) Reetz, M. T.; Kayser, F.; Harms, K. *Tetrahedron Lett.* **1992**, *33*, 3453.



**Table 2.** Photolysis of  $\Delta^1$ -Pyrazolines To Afford Cyclopropanes<sup>a</sup>

entry	pyrazoline	solvent <sup>b</sup>	photosensitizer (equiv)	time	cyclopropane	% yield <sup>c</sup>	ref
1	<i>syn</i> - <b>7</b>	acetone		4 h	<i>syn</i> - <b>15</b>	52	this work
2	<i>syn</i> - <b>8</b>	acetone		6.5 h	<i>syn</i> - <b>16</b>	46	
3	<i>syn</i> - <b>8</b>	dichloromethane	benzophenone (0.1)	1.5 h	<i>syn</i> - <b>16</b>	37	
4	<i>syn</i> - <b>10</b>	dichloromethane	benzophenone (0.1)	0.5 h	<i>syn</i> - <b>18</b>	88	
5	<i>syn</i> - <b>11</b>	dichloromethane	benzophenone (0.1)	13 min	<i>syn</i> - <b>19</b>	100	1a
6	<i>syn</i> - <b>11a</b>	dichloromethane	benzophenone (0.1)	15 min	<i>syn</i> - <b>19a</b>	100	1a
7	<i>syn</i> - <b>12</b>	dichloromethane	benzophenone (0.1)	14 min	<i>syn</i> - <b>20</b>	100	15

<sup>a</sup> Irradiations were performed with a 125-W medium-pressure mercury lamp refrigerated by circulating methanol cooled at  $-35\text{ }^\circ\text{C}$ . The whole system was refrigerated by immersion into a dry ice–acetone bath. <sup>b</sup> 0.02 M solutions were used in all cases. <sup>c</sup> Isolated yield.

mixture. Lactone **28** shows specific rotation  $[\alpha]_{\text{D}} -40$  and spectral data different from those obtained for **28a**. Moreover, selective proton irradiation of **28** gave NOE enhancements consistent with the *syn*-configuration, as depicted in Figure 2. Therefore, we must conclude that,

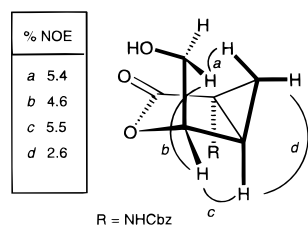


**Figure 2.** Relevant % NOE values for the stereochemical assignment of lactone **28**.

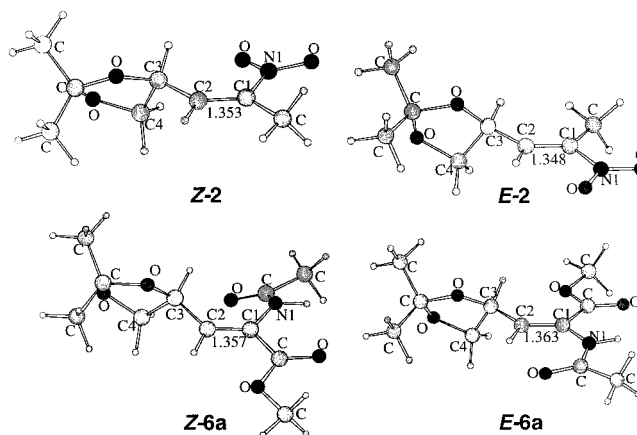
in our previous work, isomerization occurred when **20** was submitted to acid hydrolytic conditions for a long period of time. Probably, isomerization takes place on the diol intermediate since such a process had been observed on closely related substrates.<sup>1a</sup> Furthermore, some epimerization resulted when acetonide *syn*-**19** was exposed to acid for 5 days. A diastereomerically pure diol was obtained, however, when *syn*-**19** was treated with acid for 4–4.5 h.<sup>1a</sup>

Syn-stereoselectivity is, therefore, predominant in all cases independent of the substitution and the geometry of the olefins considered. These results are in good agreement with those described by Raimondi on the cycloadditions of diazomethane to several  $\gamma$ -alkoxy- $\alpha,\beta$ -unsaturated esters and diesters<sup>4g</sup> and allow us to extend her earlier conclusions to other kinds of olefins.

**2. Theoretical Calculations.** Density functional calculations were done to rationalize the  $\pi$ -facial diastereoselection in the attack of diazomethane to such chiral olefins. Nitro compounds **2** and acetyl amino pentenoates **6a** were chosen as representative systems to be studied.

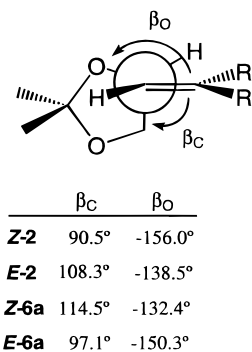
Figure 3 presents the optimized geometries of *Z* and *E* isomers of olefins **2** and **6a**. In all cases we have examined the different conformations arising from the rotation around the C2–C3 bond, and for **6a** we have also considered different conformations of the ester and acetyl amino groups. The structures presented in Figure 3 correspond to the most stable ones for each molecule.

Figure 3 shows that there are slight differences in the value of the C1–C2 bond length. This bond is longer in **6a** than in **2**. There are also differences between stereoisomers: for **2**, the C1–C2 bond is longer in the *Z* isomer, whereas for **6a** the *E* isomer presents a larger bond length. These results seem to indicate that the dioxolane group has a larger repulsion with the nitro and ester groups than with the methyl and acetyl amino groups. We can also observe that in all cases the dioxolane group



**Figure 3.** Optimized structures of olefins **2** and **6a**. Selected bond lengths in Å.

adopts an orientation in which the C3–H bond is nearly eclipsed with the C1–C2 double bond, in good agreement with the results obtained by Gung et al.<sup>16</sup> for several allyl ethers. The values of the dihedral angles corresponding to rotation around C2–C3 are shown in Figure 4.

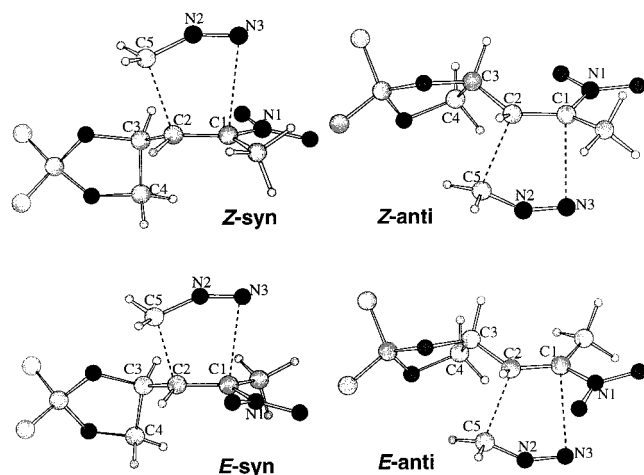


**Figure 4.** Values of the dihedral angles (in degrees) corresponding to the rotation around the C2–C3 bond for the equilibrium geometries of olefins **2** and **6a**.

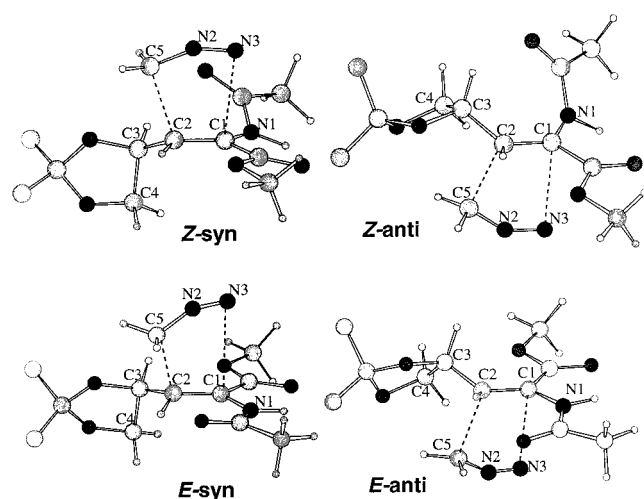
We have studied the attack of diazomethane on both isomers of olefins **2** and **6a**. In all cases, we have located transition states leading to each one of the two possible diastereoisomers, *syn* and *anti*. The corresponding transition state structures are represented in Figures 5 and 6. Table 3 presents the values of selected geometry parameters for these transition states, and the computed energy barriers are presented in Table 4.

Table 4 shows that in all cases the attack at the *syn*-face is kinetically the most favorable, in excellent agreement with the observed diastereoselectivity. The values





**Figure 5.** Structures of the transition states of the reactions between **2** and diazomethane. The hydrogen atoms of dioxolane methyl groups have been omitted for clarity.



**Figure 6.** Structures of the transition states of the reactions between **6a** and diazomethane. The hydrogen atoms of dioxolane methyl groups have been omitted for clarity.

of the  $\beta_C$  dihedral angle at the syn transition states show that the orientation of the dioxolane group in the olefin moiety is very similar to the one corresponding to the isolated molecules (see Figure 4). In this way, the syn-face is less sterically hindered. On the other hand, anti transition states can be related to the same conformation of the isolated olefins.

The values of the distances corresponding to the two forming bonds (C2–C5 and C1–N3) at the transition states of the studied reactions can be compared with the values obtained for the reaction between diazomethane and ethylene (2.301 and 2.406 Å, respectively).<sup>17</sup> We can observe that the presence of the substituents in the olefin leads to a larger asynchrony at the transition states. For the transition state of the reaction between diazomethane and ethylene it was observed that the five atoms directly involved in the cycloaddition process were coplanar. This is no longer the case for olefins **2** and **6a**, for which different degrees of deviation from planarity are observed from the values of the  $\beta_N$  dihedral angle (see Table 3).

When diazomethane attacks the syn-face of a substituted olefin, there are two different ways to minimize steric repulsion with the substituents: an counterclockwise rotation around the C2–C3 bond (see Figure 4) and torsion around the C2–C5 axis. When the attack is produced on the anti-face, the same kinds of rearrangements are observed. For the transition states of *Z*-**2**, torsion around C2–C5 moves the methylene group of diazomethane away from dioxolane and brings the N3 atom of diazomethane closer to the nitro group. The displacement from planarity is larger for the anti transition state, while the distortion corresponding to rotation around C2–C3 is smaller. On the other hand, for the transition states of *E*-**2**, torsion around C2–C5 brings the N3 atom of diazomethane closer to the methyl group. The torsion angles are smaller, indicating that the repulsion with the methyl group is larger than with the nitro group. Since the deviation from planarity is smaller, the distortion corresponding to C2–C3 rotation is larger both for syn and anti transition states (see Table 3 and Figure 5).

For the reactions of **6a** (Figure 6), torsion around C2–C5 moves the N3 atom of diazomethane away from the acetyl amino group. For *Z*-syn, this torsion brings the CH<sub>2</sub> group of diazomethane closer to the dioxolane ring, so an important torsion around C2–C3 is produced to minimize repulsion. For *Z*-anti, repulsion with dioxolane is so large that torsion around C2–C5 is very small and rotation around C3–C2 is very important. Both for *E*-syn and *E*-anti, torsion around C2–C5 moves N3 away from the acetyl amino group and the CH<sub>2</sub> group of diazomethane away from dioxolane, so that rotation around C2–C3 is less important.

The values of energy barriers presented in Table 4 show that in all cases the syn transition state is the energetically most favorable one, in excellent agreement with the experimental results. The energy barriers obtained with the TZP basis set are slightly larger than the ones corresponding to the 6-31G(d) basis set, due to a decrease in the basis set superposition error.

To discuss the origin of the facial selectivity, we will perform an energy partition for the potential energy barriers. According to the method developed by Ziegler and Rauk,<sup>18</sup> the interaction energy between two fragments,  $\Delta E$ , can be decomposed into the following terms:

$$\Delta E = \Delta E_{\text{prep}} + \Delta E_{\text{st}} + \Delta E_{\text{orb}}$$

where  $\Delta E_{\text{prep}}$ , the *preparation energy* term, is the energy necessary to distort the fragments from their equilibrium geometries to the ones they have at the transition state. The second term,  $\Delta E_{\text{st}}$ , is called the *steric energy* term and represents the interaction energy between both fragments with the geometries corresponding to the transition state, but with the densities they would have in the absence of the other fragment. Finally,  $\Delta E_{\text{orb}}$  is the *orbital interaction* term and represents the energy stabilization produced when the densities of both fragments are allowed to relax. The results of this analysis are shown in Table 5.

The preparation and steric energy terms are always larger for anti transition states than for the syn ones.

(17) Branchadell, V.; Muray, E.; Oliva, A.; Ortuño, R. M.; Rodríguez-García, C. *J. Phys. Chem. A* **1998**, *102*, 10106.

(18) (a) Ziegler, T.; Rauk, A. *Theor. Chim. Acta* **1977**, *46*, 1. (b) Ziegler, T.; Rauk, A. *Inorg. Chem.* **1979**, *18*, 1558. (c) Ziegler, T.; Rauk, A. *Inorg. Chem.* **1979**, *18*, 1755.

**Table 3. Selected Geometry Parameters<sup>a</sup> for the Transition States of the Reactions of Olefins **2** and **6a** with Diazomethane**

olefin	isomer	TS <sup>b</sup>	C2–C5	C1–N3	C1–C2	C5–N2	N2–N3	C5–N2–N3	$\beta_C^c$	$\beta_N^d$
<b>2</b>	<i>Z</i>	syn	2.171	2.629	1.400	1.344	1.159	150.7	70.3	8.4
		anti	2.155	2.679	1.401	1.343	1.159	151.4	78.0	-15.9
	<i>E</i>	syn	2.173	2.636	1.395	1.341	1.158	151.4	80.9	3.3
		anti	2.176	2.691	1.394	1.339	1.158	152.8	68.3	-7.2
<b>6a</b>	<i>Z</i>	syn	2.180	2.778	1.397	1.336	1.158	154.0	75.9	-19.0
		anti	2.120	2.730	1.406	1.346	1.162	150.0	62.0	2.4
	<i>E</i>	syn	2.147	2.837	1.402	1.339	1.162	153.0	75.4	25.1
		anti	2.154	2.849	1.401	1.338	1.162	153.8	79.5	-23.4

<sup>a</sup> Bond distances in Å and angles in degrees. <sup>b</sup> See Figures 5 and 6. <sup>c</sup> C4–C3–C2–C1 dihedral angle. <sup>d</sup> N2–C5–C2–C1 dihedral angle.

**Table 4. Potential Energy Barriers<sup>a</sup> for the Reactions of Olefins **2** and **6a** with Diazomethane Computed with Different Basis Sets**

olefin	isomer	TS <sup>b</sup>	6-31G(d)	TZP
<b>2</b>	<i>Z</i>	syn	10.2	13.0
		anti	10.9	14.4
	<i>E</i>	syn	8.7	11.6
		anti	11.6	14.3
<b>6a</b>	<i>Z</i>	syn	7.9	11.1
		anti	13.3	17.4
	<i>E</i>	syn	8.1	11.5
		anti	10.3	14.1

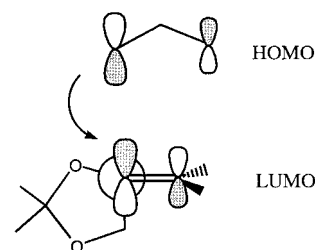
<sup>a</sup> In kcal mol<sup>-1</sup>. <sup>b</sup> See Figures 5 and 6.

Steric hindrance is larger when diazomethane approaches the anti-face. This repulsion can be relieved through geometry distortion of both fragments. The orbital interaction term is very similar for both transition states in *E-2* and *E-6a*. For *Z-2*, it is more stabilizing for the anti transition state. In this case, the value of the C2–C5 distance is shorter than for the syn transition state (see Table 3). The same kind of behavior is observed for *Z-6a*, where syn–anti differences in all contributions to the barrier are notably large. In this system, the anti transition state is clearly closer to the products in the reaction coordinate (see the values of C2–C5 and C1–N3 in Table 3) and both fragments are more distorted. As we have already said, torsion around C2–C5 is very unfavorable in this case, so the relief of steric repulsion can only be achieved through larger distortion of the fragments and by a transition state in which the degree of bond formation is higher.

Steric repulsion due to the dioxolane group plays a major role in the facial selectivity of the studied reactions. The most favorable transition states always involve attack to the less sterically hindered syn-face of the olefin. It may seem surprising that anti transition states can be also related to the same conformation of the olefin. Rotation around the C2–C3 bond would lead to a conformation in which the oxygen atom linked to C3 is antiperiplanar with respect to the incoming diazomethane molecule, and then the anti-face would be less sterically hindered. In fact, for the anti attack to *E-2*, we have located a stationary point on the potential energy surface with such an orientation of dioxolane, but this structure is 0.5 kcal mol<sup>-1</sup> higher in energy than the *E-anti* transition state presented in Figure 5.

According to the *outside alkoxy* model defined by Raimondi,<sup>48</sup> the presence of oxygen in the outside position (see Figure 7) at the transition state is favored due to the electrostatic interaction with the positively charged carbon atom of diazomethane. This interpretation would be consistent with our results, which show that in the formation of the preferred diastereoisomer, the oxygen is always in the outside position and the hydrogen is

inside. On the other hand, according to Raimondi and to the *inside alkoxy* model formulated by Houk,<sup>3</sup> the presence of the oxygen in the anti-position would not be favored since electron density from the C–C  $\pi$  orbital would be transferred to the C–O  $\sigma^*$  bond. The examination of the frontier orbitals of diazomethane and of olefins **2** and **6a** shows that the most favorable interaction is the one involving the HOMO of diazomethane and the LUMO of the olefin (see Chart 3). Thus, there is a charge

**Chart 3**

transfer from diazomethane to the olefin. The values of charge transfer at the transition states determined from Mulliken population analysis range from 0.17 to 0.22 au, being slightly larger for the reactions of **2** than for the reactions of **6a**. A conformation in which electrons are withdrawn from the C–C  $\pi$  region would favor interaction with diazomethane, but this does not seem to be the case.

We have done model calculations on two different conformations of *E-2* that differ from each other in the orientation of the dioxolane group. For these structures, we have calculated the interaction energy with an ammonia molecule placed at 2 Å from C2 in the same direction in which the carbon atom of diazomethane approaches at the anti transition state. The interaction is more favorable when the olefin has the same conformation as in the *E-anti* transition state shown in Figure 5. We have also done a similar calculation substituting ammonia by a pyramidally distorted BH<sub>3</sub> molecule. In this case, the preferred conformation is the one in which O is in the anti-position. These results seem to show that the interaction of an electron donor is not favorable when there is an oxygen atom in the anti-position.

The HOMO of olefins **2** and **6b** is an orbital with a large contribution from the p orbitals of dioxolane oxygen atoms perpendicular to the ring. When oxygen is in the anti-position, some kind of interaction with the C–C  $\pi^*$  orbital seems possible, thus interfering with the charge transfer from diazomethane (see Chart 4).

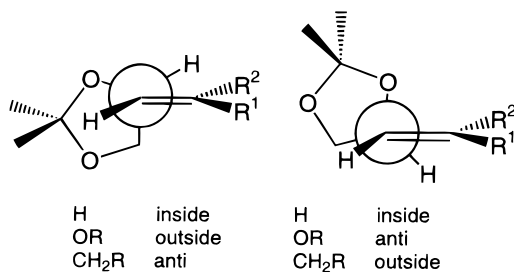
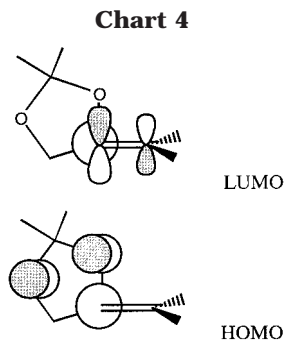
### Concluding Remarks

As a conclusion of our investigations, the stereochemical outcome of the diazomethane cycloadditions to chiral

**Table 5.** Partition of the Energy Barriers<sup>a</sup> for the Reactions of Olefins **2** and **6a** with Diazomethane

olefin	isomer	TS <sup>b</sup>	$\Delta E_{\text{prep}}$	$\Delta E_{\text{St}}$	$\Delta E_{\text{orb}}$	$\Delta E$
<b>2</b>	<i>Z</i>	syn	18.5 (0.0)	36.1 (0.0)	-41.6 (0.0)	13.0 (0.0)
		anti	19.4 (+0.9)	38.9 (+2.8)	-43.9 (-2.3)	14.4 (+1.4)
	<i>E</i>	syn	17.4 (0.0)	35.6 (0.0)	-41.4 (0.0)	11.6 (0.0)
		anti	19.3 (+1.9)	36.2 (+0.6)	-41.2 (+0.2)	14.3 (+2.7)
<b>6a</b>	<i>Z</i>	syn	15.3 (0.0)	35.0 (0.0)	-39.2 (0.0)	11.1 (0.0)
		anti	21.9 (+6.6)	42.0 (+7.0)	-46.5 (-7.3)	17.4 (+6.3)
	<i>E</i>	syn	15.1 (0.0)	38.0 (0.0)	-41.6 (0.0)	11.5 (0.0)
		anti	16.9 (+1.8)	39.0 (+1.0)	-41.8 (-0.2)	14.1 (+2.6)

<sup>a</sup> Energies computed with the TZP basis set in kcal mol<sup>-1</sup>. See the text for definitions. In parentheses are values relative to the syn transition state. <sup>b</sup> See Figures 5 and 6.

**Figure 7.** Possible conformations of olefins **2** and **6a** arising from the rotation around the C2–C3 bond.

$\gamma$ -alkoxy olefins, bearing different electron-withdrawing substituents conjugated to the double bond, has been established and rationalized.

Single-crystal X-ray structural analysis and NMR experiments confirm *syn* diastereoselection to be preferred, independently of the *Z/E* stereochemistry of the substrate, the mono- or disubstitution at the olefinic C1 position, and the nature of the conjugated functional groups.

Theoretical calculations allow us to state the main role played by the dioxolane ring in the diastereoselection. Thus, steric factors account mainly for the diazomethane preferential *syn*-attack to all studied olefins.

Therefore, as a general conclusion, the origin of the  $\pi$ -facial diastereoselection in these cycloadditions is found in the chirality of the dioxolane stereogenic center, as the most relevant feature determining the stereochemistry of the resulting adducts.

### Experimental Section

Flash column chromatography was carried out on silica gel (240–400 mesh). Melting points were determined on a hot stage and are uncorrected. Distillation of small amounts of material was effected in a bulb-to-bulb distillation apparatus, with oven temperatures (ot) being reported. Electron impact mass spectra were recorded at 70 eV. Chemical shifts in NMR spectra are given on the  $\delta$  scale.

Olefins *Z*- and *E*-**2**,<sup>8</sup> *Z*-**9** and *E*-**3**,<sup>10</sup> *Z*- and *E*-**4**,<sup>11</sup> *Z*-**12** and *E*-**5**,<sup>13</sup> and *E*-**6**,<sup>14</sup> and compounds *syn*-**12**, and *syn*-**20**<sup>15</sup> were

prepared according to protocols described in the literature, their spectroscopic data and physical constants being in good agreement with those previously reported for such products.

**Computational Details.** All calculations have been done using density functional (DFT) methods within the generalized gradient approximation (GGA). Molecular geometries have been fully optimized using Becke's<sup>19</sup> functional for exchange and the correlation functional due to Perdew and Wang<sup>20</sup> (BPW91). This functional has been shown to yield excellent results for the addition of diazomethane to ethylene.<sup>17</sup> Molecular geometries have been fully optimized at this level of calculation using the standard 6-31G(d) basis set.<sup>21</sup> Stationary points have been characterized as energy minima or transition states through the calculations of the energy second derivatives. These calculations have been done with the Gaussian 94 program.<sup>22</sup> Single point calculation have been done for the previously optimized geometries using an uncontracted Slater type orbital (STO) triple- $\zeta$  basis set supplemented with a set of *d* polarization functions for C, N, and O, and with a set of *p* functions for H (TZP).<sup>23</sup> These calculations have been done using the ADF program.<sup>24</sup>

**General Procedure for the Cycloadditions of Diazomethane to Olefins **2**, **3**, **5**, and **6**.** A typical experiment is described for the synthesis of pyrazoline *syn*-**7**. An ethereal solution of excess diazomethane was distilled onto *Z*-**1** (307 mg, 1.6 mmol) in 10 mL of ether, at 0 °C. The light-protected resultant solution was stirred at 0 °C for 1 h, then excess diazomethane was destroyed by addition of CaCl<sub>2</sub>, and solvent was removed. The residue was chromatographed on silica gel (1:3 EtOAc–hexane) to afford pure *syn*-**7**, which was crystallized from EtOAc–pentane. The new pyrazolines *syn*-**8**, *anti*-**8**, *syn*-**9**, *syn*-**10**, and **13** and known *syn*-**12**<sup>15</sup> were prepared in a similar manner.

**(3*R*,4*R*,4'*S*)-4-(2',2'-Dimethyl-1',3'-dioxol-4'-yl)-3-methyl-3-nitro-1,2-pyrazoline, *syn*-**7**:** yield, 280 mg (75%); crystals, mp 93–95 °C (from EtOAc–pentane);  $[\alpha]_D^{25} +192.5$  (c 0.8, CHCl<sub>3</sub>); IR (KBr) 1557, 1382 cm<sup>-1</sup>; 250-MHz <sup>1</sup>H NMR (CDCl<sub>3</sub>) 1.24 (s, 3H), 1.35 (s, 3H), 2.00 (s, 3H), 2.14 (ddd, *J* = *J* = *J*' = 8.0 Hz, 1H), 3.60 (dd, *J* = 8.0 Hz, *J*' = 5.1 Hz, 1H), 3.77 (m, 1H), 3.98 (dd, *J* = 8.0 Hz, *J*' = 5.8 Hz, 1H), 4.66 (dd, *J* = 18.0 Hz, *J*' = 8.0 Hz, 1H), 4.97 (dd, *J* = 18.0 Hz, *J*' = 8.0 Hz, 1H); 62.5-MHz <sup>13</sup>C NMR (CDCl<sub>3</sub>) 22.63, 24.92, 26.57, 46.06, 67.83,

(19) Becke, A. D. *Phys. Rev. A* **1988**, *38*, 3098.

(20) (a) Wang, Y.; Perdew, J. P. *Phys. Rev. B* **1991**, *44*, 13298. (b) Perdew, J. P.; Chevary, J. A.; Vosko, S. H.; Jackson, K. A.; Pederson, M. R.; Singh, D. J.; Fiolhais, C. *Phys. Rev. B* **1992**, *46*, 6671.

(21) Hehre, W. J.; Radom, L.; Schleyer, P. v. R.; Pople, J. A. *Ab Initio Molecular Orbital Theory*; Wiley: New York, 1986.

(22) Frisch, M. J.; Trucks, G. W.; Schlegel, H. B.; Gill, P. M. W.; Johnson, B. G.; Robb, M. A.; Cheeseman, J. R.; Keith, T. A.; Petersson, G. A.; Montgomery, J. A.; Raghavachari, K.; Al-Laham, M. A.; Zakrzewski, V. G.; Ortiz, J. V.; Foresman, J. B.; Cioslowski, J.; Stefanov, B. B.; Nanayakkara, A.; Challacombe, M.; Peng, C. Y.; Ayala, P. Y.; Chen, W.; Wong, M. W.; Andrés, J. L.; Replogle, E. S.; Gomperts, R.; Martin, R. L.; Fox, D. J.; Binkley, J. S.; Defrees, D. J.; Baker, J.; Stewart, J. J. P.; Head-Gordon, M.; Gonzalez, C.; Pople, J. A. *Gaussian 94*, Revision B.3; Gaussian Inc.: Pittsburgh, PA, 1995.

(23) Vernooijs, P.; Snijders, G. J.; Baerends, E. J. *Slater Type Basis Functions for the whole Periodic System*; Internal Report, Freie Universiteit Amsterdam, The Netherlands, 1981.

(24) (a) ADF 2.3, Theoretical Chemistry, Vrije Universiteit, Amsterdam. (b) Baerends, E. J.; Ellis, D. E.; Ros, P. *Chem. Phys.* **1973**, *2*, 41. (c) Velde, G.; Baerends, E. J. *J. Comput. Phys.* **1992**, *99*, 84.



74.00, 80.79, 109.41, 119.52. Anal. Calcd for  $C_9H_{15}N_3O_4$ : C, 47.16; H, 6.59; N, 18.33. Found C, 47.49; H, 6.68; N, 18.89.

**(3S,4R,4'S)-4-(2',2'-Dimethyl-1',3'-dioxol-4'-yl)-3-methyl-3-nitro-1,2-pyrazoline, syn-8**: yield, 600 mg (76%); crystals, mp 50–53 °C (from EtOAc–pentane);  $[\alpha]_D -448.0$  (*c* 0.86,  $CHCl_3$ ); IR (KBr) 1539, 1380  $cm^{-1}$ ; 250-MHz  $^1H$  NMR ( $CDCl_3$ ) 1.27 (s, 3H), 1.35 (s, 3H), 2.01 (s, 3H), 2.64 (ddd, *J* = 6.8 Hz, *J*' = 3.5 Hz, 1H), 3.52 (dd, *J* = 8.4 Hz, *J*' = 6.6 Hz, 1H), 4.10 (dd, *J* = 8.4 Hz, *J*' = 6.6 Hz, 1H), 4.22 (ddd, *J* = *J*' = 6.6 Hz, *J*'' = 3.5 Hz, 1H), 4.83 (d, *J* = 6.8 Hz, 2H); 62.5-MHz  $^{13}C$  NMR ( $CDCl_3$ ) 17.39, 24.80, 26.02, 42.82, 68.10, 72.18, 78.66, 110.13, 123.30. Anal. Calcd for  $C_9H_{15}N_3O_4$ : C, 47.16; H, 6.59; N, 18.33. Found C, 46.83; H, 6.72; N, 18.18.

**(3R,4S,4'S)-4-(2',2'-Dimethyl-1',3'-dioxol-4'-yl)-3-methyl-3-nitro-1,2-pyrazoline, anti 8**: yield, 40 mg (5%); crystals, mp 94–95 °C (from EtOAc–pentane);  $[\alpha]_D +363.1$  (*c* 1.26,  $CHCl_3$ ); IR (KBr) 1558, 1378  $cm^{-1}$ ; 250-MHz  $^1H$  NMR ( $CDCl_3$ ) 1.29 (s, 3H), 1.31 (s, 3H), 1.85 (s, 3H), 2.92 (ddd, *J* = *J*' = *J*'' = 8.8 Hz, 1H), 3.56 (dd, *J* = 8.0 Hz, *J*' = 5.1 Hz, 1H), 3.03 (m, 3H), 4.92 (dd, *J* = 17.6, *J*' = 8.8 Hz, 1H); 62.5-MHz  $^{13}C$  NMR ( $CDCl_3$ ) 15.97, 25.24, 26.42, 45.12, 68.15, 73.74, 77.97, 110.26, 124.03. Anal. Calcd for  $C_9H_{15}N_3O_4$ : C, 47.16; H, 6.59; N, 18.33. Found C, 47.04; H, 6.64; N, 18.25.

**(3R,4R,4'S)-4-(2',2'-Dimethyl-1',3'-dioxol-4'-yl)-3-ethoxy-carbonyl-3-methyl-1,2-pyrazoline, syn-9**: yield, 266 mg (90%); crystals, mp 49–51 °C (from EtOAc–pentane);  $[\alpha]_D +132.3$  (*c* 0.94,  $CHCl_3$ ); IR (KBr) 1722  $cm^{-1}$ ; 250-MHz  $^1H$  NMR ( $CDCl_3$ ) 1.23 (t, *J* = 7.3 Hz, 3H), 1.24 (s, 3H), 1.32 (s, 3H), 1.61 (s, 3H), 1.90 (q, *J* = 8.4 Hz, 1H), 3.52 (m, 1H), 3.93 (m, 2H), 4.15 (m, 2H), 4.44 (dd, *J* = 18.0 Hz, *J*' = 8.4 Hz, 1H), 4.81 (dd, 2H, *J* = 18.0 Hz, *J*' = 0.4 Hz, 1H); 62.5-MHz  $^{13}C$  NMR ( $CDCl_3$ ) 13.94, 22.53, 25.18, 26.53, 47.03, 61.79, 68.27, 74.50, 79.18, 92.53, 109.03, 169.00. Anal. Calcd for  $C_{12}H_{20}N_2O_4$ : C, 56.23; H, 7.87; N, 10.93. Found C, 56.36; H, 7.67; N, 11.06.

**(3S,4'S)-4-(2',2'-Dimethyl-1',3'-dioxol-4'-yl)-3-ethoxy-carbonyl-3-methyl-1,2-pyrazoline, syn-10**: yield, 340 mg (71%); oil; IR (film) 1736  $cm^{-1}$ ; 250-MHz  $^1H$  NMR ( $CDCl_3$ ) 1.27 (t, *J* = 7.3 Hz, 3H), 1.29 (s, 3H), 1.36 (s, 3H), 1.56 (s, 3H), 2.41 (m, 1H), 3.52 (m, 1H), 4.06 (m, 2H), 4.21 (q, *J* = 7.3), 4.65 (m, 2H); 62.5-MHz  $^{13}C$  NMR ( $CDCl_3$ ) 13.96, 16.12, 25.15, 26.33, 41.24, 62.00, 68.44, 73.74, 78.47, 93.94, 109.35, 170.88. Anal. Calcd for  $C_{12}H_{20}N_2O_4$ : C, 56.23; H, 7.87; N, 10.93. Found C, 56.18; H, 7.93; N, 11.25.

**(4R,4'S)-4-(2',2'-Dimethyl-1',3'-dioxolan-4'-yl)-3-(phenylsulfonyl)-4,5-dihydro-1H-pyrazole, 13**: yield, (a) from **Z-3**, 486 mg (70%); (b) from **E-3**, 564 mg (75%); solid, mp 150–152 °C (dec);  $[\alpha]_D +22.9$  (*c* 0.88,  $CHCl_3$ ); IR (KBr) 3360, 1532, 1145  $cm^{-1}$ ; 250-MHz  $^1H$  NMR ( $CDCl_3$ ) 1.23 (s, 3H), 1.34 (s, 3H), 3.55 (m, 1H), 3.77 (m, 3H), 4.14 (dd, *J* = 8.8 Hz, *J*' = 6.5 Hz, 1H), 4.46 (dt, *J* = 12.0 Hz, *J*' = 6.5 Hz, 1H), 7.57 (m, 3H), 7.95 (m, 2H); 62.5-MHz  $^{13}C$  NMR 24.94, 26.39, 48.18, 51.77, 68.41, 73.47, 109.32, 128.29, 129.03, 133.70, 139.61, 150.11. Anal. Calcd for  $C_{14}H_{18}N_2O_4S$ : C, 54.18; H, 5.84; N, 9.03; S, 10.33. Found C, 54.33; H, 5.71; N, 8.89; S, 10.20.

**General Procedure for the Photolysis of Pyrazolines syn-7, syn-8, syn-10, syn-12, and 13**. In a typical experiment, a 0.02 M solution of pyrazoline contained in a Pyrex reactor under nitrogen atmosphere was irradiated with a 125 W medium-pressure mercury lamp refrigerated by circulating methanol cooled at –35 °C. The whole system was cooled by immersion into a dry ice–acetone bath. Solvent, photosensitizer, and reaction time for each case is shown in Table 1. The reaction progress was monitored by UV ( $\lambda_{max}$  = 323–328 nm for **syn-7**, **syn-8**, and **syn-10**, and 410 nm for **syn-12**). When total conversion was accomplished, solvent was removed and the residue was chromatographed (EtOAc–hexane mixtures) to afford the new cyclopropanes **syn-15**, **syn-16**, and **syn-18** and the already known **syn-20**.<sup>15</sup>

**(1S,2R,4'S)-2-(2',2'-Dimethyl-1',3'-dioxol-4'-yl)-1-methyl-1-nitrocyclopropane, syn-15**: yield, 106 mg (52%); oil  $[\alpha]_D +20.1$  (*c* 0.82,  $CHCl_3$ ); IR (film) 1536, 1362  $cm^{-1}$ ; 250-MHz  $^1H$  NMR ( $CDCl_3$ ) 1.35 (m, 2H), 1.30 (s, 3H), 1.42 (s, 3H), 1.73 (s, 3H), 2.12 (t, *J* = 7.3 Hz, 1H), 3.61 (m, 1H), 3.95 (m, 2H); 62.5-MHz  $^{13}C$  NMR ( $CDCl_3$ ) 21.14, 21.19, 25.33, 26.79, 32.61, 65.00,

68.82, 74.59, 109.24; HRMS (EI) *m/z* calcd for  $C_8H_{12}NO_4$  186.0766 (*M* – 15), found 186.0768 (*M* – 15).

**(1R,2R,4'S)-2-(2',2'-Dimethyl-1',3'-dioxol-4'-yl)-1-methyl-1-nitrocyclopropane, syn-16**: yield, 97 mg (46%); oil, ot 60 °C (0.1 Torr);  $[\alpha]_D -87.7$  (*c* 1.75,  $CHCl_3$ ); IR (film) 1539, 1356  $cm^{-1}$ ; 250-MHz  $^1H$  NMR ( $CDCl_3$ ) 1.22 (dd, *J* = 7.7 Hz, *J*' = 5.5 Hz, 1H), 1.31 (s, 3H), 1.38 (s, 3H), 1.73 (s, 3H), 2.00 (dd, *J* = 7.7 Hz, *J*' = 5.5 Hz, 1H), 2.17 (m, 1H), 3.70 (dd, *J* = 8.4 Hz, *J*' = 6.5 Hz, 1H), 3.92 (ddd, *J* = *J*' = *J*'' = 6.5 Hz, 1H), 4.12 (dd, *J* = 8.4 Hz, *J*' = 6.5 Hz, 1H); 62.5-MHz  $^{13}C$  NMR ( $CDCl_3$ ) 14.93, 21.28, 25.68, 26.35, 31.76, 63.05, 69.29, 73.47, 109.74. Anal. Calcd for  $C_9H_{15}NO_4$ : C, 53.72; H, 7.51; N, 6.96. Found C, 53.57; H, 7.44; N, 6.97.

**Ethyl (1R,2R,4'S)-1-methyl-2-(2',2'-dimethyl-1',3'-dioxolan-4'-yl)cyclopropane carboxylate, syn-18**: yield, 200 mg (88%); oil, ot 60 °C (0.01 Torr);  $[\alpha]_D -41.5$  (*c* 2.14,  $CHCl_3$ ); IR (film) 1722  $cm^{-1}$ ; 250-MHz  $^1H$  NMR ( $CDCl_3$ ) 0.78 (dd, *J* = 6.6 Hz, *J*' = 4.4 Hz, 1H), 1.19 (t, *J* = 6.6, 3H), 1.26 (s, 3H), 1.32 (s, 3H), 1.40 (s, 3H), 1.44 (m, 1H), 1.57 (m, 1H), 3.64 (t, *J* = 7.3 Hz, 1H), 3.75 (q, *J* = 7.3 Hz, 1H), 4.05 (m, 3H); 62.5-MHz  $^{13}C$  NMR ( $CDCl_3$ ) 14.09, 14.54, 20.80, 21.97, 25.77, 26.63, 28.37, 60.73, 69.43, 76.25, 109.02, 174.95. Anal. Calcd for  $C_{12}H_{20}O_4$ : C, 63.14; H, 8.83. Found C, 62.98; H, 8.93.

**Hydrolysis of Acetonides syn-15, syn-16, syn-18, and syn-20**. A methanolic solution of acetonide containing some drops of aqueous 5% HCl was stirred at room temperature for 4–5 h in the case of **syn-15**, **syn-16**, **syn-18** and 1.5 h in the case of **syn-20**, until consumption of the starting material (TLC monitoring). Solvent was removed at reduced pressure and the crude product was purified by column chromatography on silica gel (EtOAc–hexane mixtures). Diols **21**, **22**, and **23** and hydroxy lactone **28** were thus obtained.

**(1S,2R,1'S)-1-Methyl-1-nitro-2-(1',2'-dihydroxyethyl)cyclopropane, 21**: yield, 70 mg (95%); crystals, mp 43–45 °C (from EtOAc–pentane);  $[\alpha]_D +19.1$  (*c* 0.31,  $CHCl_3$ ); IR (KBr) 3700–3050 (broad), 1533, 1391  $cm^{-1}$ ; 250-MHz  $^1H$  NMR ( $CDCl_3$ ) 1.29 (dd, *J* = 9.5 Hz, *J*' = 6.3 Hz, 1H), 1.49 (ddd, *J* = *J*' = 9.5 Hz, *J*'' = 1.5 Hz, 1H), 1.75 (s, 3H), 2.16 (t, *J* = 6.3 Hz, 1H), 3.55 (m, 3H), 2.3 and 2.7 (broad, OH); 62.5-MHz  $^{13}C$  NMR ( $CDCl_3$ ) 20.31, 21.03, 32.09, 65.74, 65.86, 69.79. Anal. Calcd for  $C_6H_{11}NO_4$ : C, 44.72; H, 6.83; N, 8.70. Found C, 44.73; H, 7.00; N, 8.65.

**(1R,2R,1'S)-1-Methyl-1-nitro-2-(1',2'-dihydroxyethyl)cyclopropane, 22**: yield, 67 mg (84%); crystals, mp 64–66 °C (from EtOAc–pentane);  $[\alpha]_D -52.9$  (*c* 1.16, MeOH); IR (KBr) 3332, 1532, 1363  $cm^{-1}$ ; 250-MHz  $^1H$  NMR (MeOH-*d*<sub>4</sub>) 1.22 (dd, *J* = 10.0 Hz, *J*' = 5.9 Hz, 1H), 1.77 (s, 3H), 1.93 (dd, *J* = 10.0 Hz, *J*' = 5.1 Hz, 1H), 2.18 (m, 1H), 3.45 (m, 1H), 3.57 (d, *J* = 5.1 Hz, 2H); 62.5-MHz  $^{13}C$  NMR (MeOH-*d*<sub>4</sub>) 16.33, 23.04, 34.32, 65.79, 67.86, 72.11. Anal. Calcd for  $C_6H_{11}NO_4$ : C, 44.72; H, 6.83; N, 8.70. Found C, 44.60; H, 6.66; N, 8.47.

**(1R,2R,1'S)-1-Ethoxycarbonyl-1-methyl-2-(1',2'-dihydroxyethyl)cyclopropane, 23**: yield, 160 mg (94%); oil unsuitable for  $[\alpha]_D$  determination and for microanalysis; IR (film) 3395 (broad), 1715  $cm^{-1}$ ; 250-MHz  $^1H$  NMR ( $CDCl_3$ ) 0.72 (dd, *J* = 6.6 Hz, *J*' = 3.7 Hz, 1H), 1.19 (t, *J* = 7.0 Hz, 3H), 1.26 (s, 3H), 1.35 (dd, *J* = 9.5 Hz, *J*' = 3.7 Hz, 1H), 1.49 (m, 1H), 3.33–3.64 (complex absorption, 5H), 4.04 (q, *J* = 7.0 Hz, 2H); 62.6-MHz  $^{13}C$  NMR ( $CDCl_3$ ) 14.03, 14.30, 20.06, 22.53, 27.94, 60.85, 66.56, 71.94, 175.35; MS, *m/z* (%) 189 (*M* + 1, 1), 157 (16), 143 (22), 111 (100), 83 (96), 55 (47).

**(1R,4S,5R)-1-(N-Benzoyloxycarbonylamino)-4-hydroxymethyl-3-oxabicyclo[3.1.0]hexan-2-one, 28**: yield, 87 mg (80%); oil;  $[\alpha]_D -40.1$  (*c* 0.76,  $CHCl_3$ ); IR (film) 3100–3690 (broad), 1778, 1715  $cm^{-1}$ ; 400-MHz  $^1H$  NMR (DMSO-*d*<sub>6</sub>) 1.31 (dd, *J* = 8.0, *J*' = 5.2, 1H); 1.37 (dd, *J* = 5.9, *J*' = 5.9, 1H); 2.27 (m, 1H), 3.14 (broad s, 1H), 3.47 (m, 1H), 4.57 (m, 1H), 4.92 (m, 1H), 5.02 (s, 2H), 7.33 (m, 5H);  $^{13}C$  NMR (acetone-*d*<sub>6</sub>) 15.10, 26.09, 39.30, 62.44, 67.06, 78.77, 128.68, 129.15, 137.56, 157.32, 174.41.

**Ethyl (1R,2R,4'S)-1-Methyl-2-(1',3'-dioxolan-2'-thioxo-4'-yl)cyclopropane carboxylate, 26**. A mixture of diol **23** (160 mg, 0.8 mmol) and *N,N*-thiocarbonyldiimidazole (336 mg, 1.7 mmol) in anhydrous THF was heated at 60 °C for 7.5 h, under nitrogen atmosphere. Solvent was removed at reduced



pressure and the residue was chromatographed on silica gel (2:1 EtOAc–hexane as eluent) to give pure **26** (106 mg, 55% yield) as a pale-yellow oil (ot 190 °C, 0.01 Torr):  $[\alpha]_D -70.6$  (c 1.18, CHCl<sub>3</sub>); IR (film) 1715 cm<sup>-1</sup>; 250-MHz <sup>1</sup>H NMR (CDCl<sub>3</sub>) 0.94 (dd, *J* = 6.0 Hz, 1H), 1.22 (t, *J* = 7.3 Hz, 3H), 1.32 (s, 3H), 1.58 (dd, *J* = 8.8 Hz, *J* = 6.0 Hz, 1H), 1.82 (m, 1H), 4.10 (q, *J* = 7.3 Hz, 2H), 4.41 (t, *J* = 8.0 Hz, 1H), 4.64 (q, *J* = 8.0 Hz, 1H), 4.75 (t, *J* = 8.0 Hz, 1H); 62.5-MHz <sup>13</sup>C NMR (CDCl<sub>3</sub>) 14.06, 14.51, 20.62, 22.83, 27.15, 61.32, 73.56, 82.38, 173.55, 191.31. Anal. Calcd for C<sub>10</sub>H<sub>14</sub>O<sub>4</sub>S: C, 52.16; H, 6.13; S, 13.92. Found C, 52.27; H, 6.11; S, 14.17.

**Acknowledgment.** E.M. thanks the Ministerio de Educación for a predoctoral fellowship. Financial support from DGEIC through the project PB97-0214 is gratefully acknowledged.

**Supporting Information Available:** Crystal data, refinement details, atomic coordinates, thermal parameters, distances, and angles for structures *syn*-**9**, **21**, and **22**. This material is available free of charge via the Internet at <http://pubs.acs.org>.

JO991227J